Acta Cryst. (1964). **17**, 569

Etching of Topaz Cleavages

By A. R. Patel and K. N. Goswami

Physics Department, Sardar Vallabhbhai Vidyapeeth, Vallabh Vidyanagar, India

(*Received* 27 *May* 1963)

Topaz cleavages have been etched in potassium hydroxide at various temperatures. Three distinctive types of distribution of etch-pits, for example (*a*) individual isolated pits, (*b*) random distribution of micro-pits and (*c*) rectilinear etch patterns, have been observed. The structure of the individual isolated pits has been investigated in detail; they are of two types, (*a*) point-bottomed and (*b*) curl-bottomed. The structures of the pits persist on continued etching. From the asymmetry of the point bottoms of the point-bottomed pits, it is established that these pits nucleate at linear dislocation lines inclined to the cleavage face at an angle of about 25°. It is conjectured that curl-bottomed pits nucleate at screw dislocations. By etching matched cleavage faces, correspondence in regard to number, shape, size, position and structure of the pits has been established. Correspondence exists even in the etch patterns on the opposite sides of thin flakes of topaz. The rectilinear etch patterns show a considerable amount of displacement when crossing large cleavage steps. The rectilinear traces are traces of planes inclined at an angle of about 45° with the cleavage face. It is, therefore, conjectured that they may be the traces of (111) planes which make an angle of about 45° with the (001) cleavage face. The correspondence in the rectilinear etch patterns on the two sides of a thin flake shows that these planes go right through the body of the crystal. The implications are discussed.

Introduction

It is an established fact that if crystal surfaces are treated with suitable solvents, the surfaces are frequently attacked locally to give small depressions called 'etch-pits'. The etching methods have now become increasingly important in revealing the sites of imperfections and in studying their types and their density in crystals. The etch patterns of certain crystals sometimes even reveal the history of their growth. The structures of the pits nucleated at dislocation sites are strictly related to the types of dislocation. Thus Gilman & Johnston (1956), from the structure of the pits produced on lithium fluoride crystals, have been able to index the edge and screw dislocations and have shown the inclination of the dislocations. Patel (1961), from the structure of the pits produced on diamond cleavages, has shown that, in diamond, dislocation lines are inclined to the cleavage faces at an angle of about 70°. Patel & Ramanathan (1962) have observed a relative displacement in the etch patterns on the two sides of a thin mica flake and have attributed this to the inclination of dislocation lines. Patel & Tolansky (1957), by etching cleaved-out blocks of diamond, have shown in a striking manner that the stratigraphical etch patterns reveal the whole growth history of diamond. Patel & Goswami (1962*a*,*b*) from the studies of stratigraphical etch patterns on calcite have attributed the growth of calcite to layer deposition on the rhombohedral faces. Gevers (1953) has made microscopic and interferometric observations of corrosion figures on topaz and has interpreted them in terms of dislocations. The method of etching is also largely used in the study of damage of crystals by radiation bombardment (Billington & Crawford, 1961).

In the present investigation a comprehensive study is made of the etch patterns on (001) cleavages of topaz crystals. These investigations are developed in three stages. First, studies are made on the etch patterns of isolated cleavages; secondly, on oppositely etched matched pairs and thirdly, on the opposite sides of a thin flake. New information regarding the nature of dislocations and the history of growth of topaz has been secured.

Experimental

We have at our disposal a white transparent topaz crystal obtained from the Geological Department of Birla Vishwakarma Mahavidyalaya, Vallabh Vidyanagar. The crystal was cleaved along the (001) basal cleavage with a sharp chisel in the laboratory. The cleavage surfaces before etching were thoroughly cleaned with distilled water and examined microscopically and interferometrically after deposition of silver films over them to enhance contrasts. The structural features were recorded. Thus Fig. 1 is a multiple-beam interferogram revealing the structure of a cleavage face of topaz. The cleavage lines are clearly revealed and the region between the two cleavage lines is quite flat. The cleavages were then etched in a melt of potassium hydroxide in a nickel crucible at different temperatures for different periods, the temperature and time of etching being adjusted by preliminary experiments. The etched surfaces were then cleaned, silvered and examined by microscopy, by multiple beam interferometry (Tolansky, 1948), and by light profile microscopy (Tolansky, 1952).

Etch pattern on topaz (001) cleavages

As in the case of other mineral crystals, there is a quite distinctive distribution of etch pits on topaz cleavages. These distributions, as shown by Patel & Tolansky (1957) on diamond surfaces are of three kinds:

(*a*) Random distribution of small micro-pits.
(*b*) Individual isolated pits, usually somewhat larger than the others yet all more or less of similar size.
(*c*) Striking linear etch patterns.

The sizes of the pits in groups (*a*) and (*b*) are quite uniform throughout each group, but in group (*c*) the pits interfere with each other and produce linear etch patterns. Fig. 2 is a fine example of type (*c*) produced by etching a topaz cleavage for 20 seconds at 400 °C. The linear etch pattern revealing the stratigraphical character of the crystal will be discussed later in detail. Fig. 3 is an example of a combination of type (*a*), random distribution, and type (*b*), individual isolated pits produced by etching at temperature below 400 °C. The random distribution of micro-pits, individual isolated pits and the small areas resistant to etch are revealed. If the crystal is etched at a temperature above 400 °C, the small randomly distributed micro-pits observed in Fig. 3 interfere with each other and are washed away, with the result that only the individual isolated pits as observed in Fig. 4 remain. It appears from Fig. 4 that the surface is attacked by the etchant at a few isolated points only where the pits are nucleated, and the rest of the surface is not attacked at all. That this is not so is clearly revealed by the interferogram of Fig. 5 which has been taken on the etched surface of topaz etched at 450 °C. When this interferogram is compared with the interferogram of Fig. 1, it reveals a striking contrast. It is clear from the interferogram of Fig. 5 that the surface has undergone a general dissolution, and that at the same time preferential attack has taken place at isolated points resulting in individual isolated pits. Thus the attack is twofold. It is, however, the careful study of the individual isolated pits which has revealed the most striking information. With regard to the individual isolated pits of Figs. 2, 3 and 4, it is observed that:

(1) The pits are strictly crystallographically oriented in (110) directions.
(2) They all have an elongated pyramidal shape. The elongated pyramid has one pair of obtuse angles of about 135°, the other pair of acute angles being acute, about 45°.
(3) The pits are point-bottomed and have a pyramidal structure.
(4) The pits are of different sizes.
(5) The pits are symmetrical about the longer diagonal but not about the shorter diagonal.
(6) The point-bottoms of the pyramidal pits are not quite symmetrical with respect to the boundary of the pits.
(7) Careful investigation of the point-pyramidal structure has revealed that the pyramidal structures also differ in the case of some pits. The pit marked *A* in Fig. 4 has a structure quite different from that of the pit marked *B*. The longer diagonal of pit *A* has a little bend near the intersection of the two diagonals of the pits. This gives a curl-bottom structure to the pits, and such pits henceforth will be described as curl-bottomed pits. The curl-bottoms of some pits are clearly revealed in subsequent photographs, for example Fig. 7, 8*a*, 8*b* and 8*c*.
(8) Some of the pits have their sides extended in the crystallographic directions, giving the appearance of wings.

The structure of pits *B* and *A* (Fig. 4) is clearly revealed in Figs. 6 and 7 respectively. In these figures the vertical black lines are the multiple-beam light profiles (Tolansky, 1952) revealing the depth of the pit at various places. It is observed that the depth of the point-bottomed pit is maximum at the point bottom, but the maximum depth of the curl-bottomed pit is at the bend of the diagonal. The depth of the pits computed from the light profile measurements of Fig. 6 is 7 μ and that of the Fig. 7 is 11·2 μ. Careful examination of Fig. 7 reveals that the light profile also runs across the wings of the pit. The profile clearly indicates that the wings are depressions and their slope is uniform. The depression of the wing is maximum on the pit side, indicating that the wing is sloping towards the pit.

In order to find out the reasons for the etch pattern described above, a topaz cleavage was selected and was etched successively for 30, 60 and 90 seconds. After each period of etching it was removed from the melt for examination. Thus etching for 30 seconds led to Fig. 8(*a*), etching for 60 seconds led to Fig. 8(*b*), and etching for 90 seconds led to Fig. 8(*c*). Attention is drawn to the following features in these figures:

(*a*) The sizes of the pits increase with increase in the time of etch, while their shape is not affected.
(*b*) An established point-pyramidal pit continues to be point-pyramidal and a curl-bottomed pit continues to remain the same, *i.e.* the structures of the pits do not change on continued etching.
(*c*) The symmetry observed in case of point-pyramidal pits, described before, increases with the time of etching.
(*d*) The bend observed in the diagonal in the case of curl-bottomed pits persists with increase in the time of etching.
(*e*) The wing structure of the pits persists on continued etching.
(*f*) It is observed that the bend in the diagonal of a curl-bottomed pit is in either direction, and it continues in the same direction with successive etching.

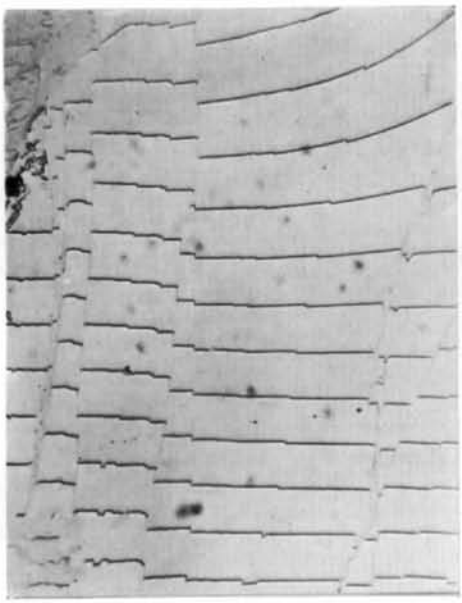

Fig. 1. Interferogram on a cleavage face of topaz.

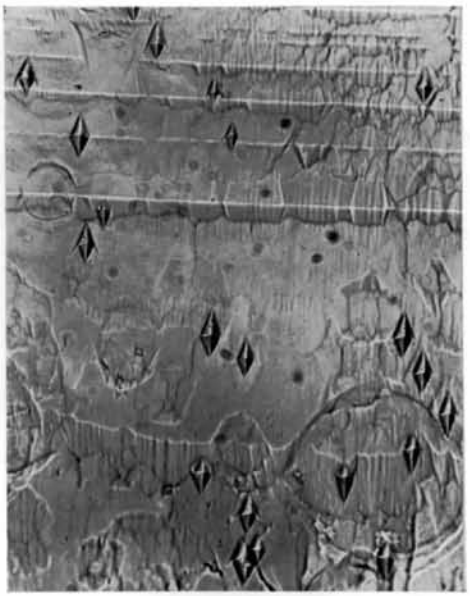

Fig. 2. A region showing rectilinear etch patterns.

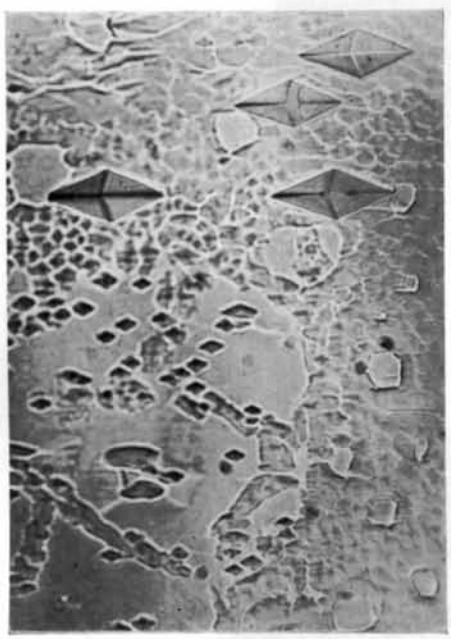

Fig. 3. Micropits and individual isolated pits.

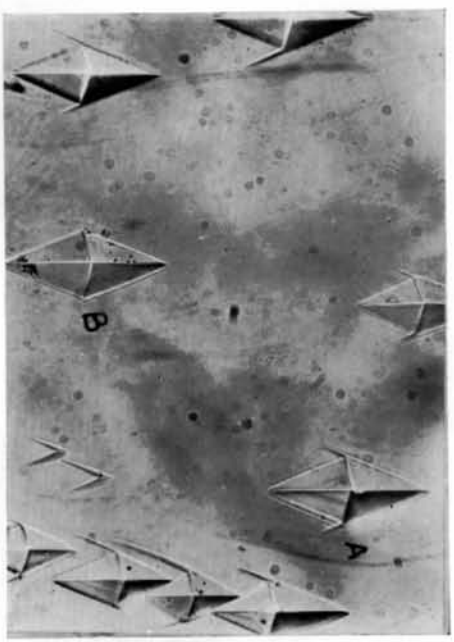

Fig. 4. A region showing only individual isolated pits.

[To face p. 570

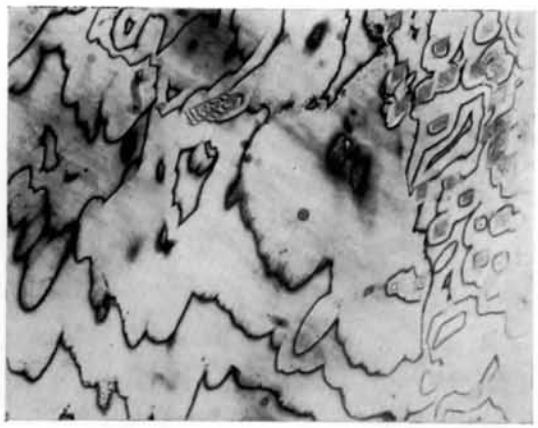

Fig. 5. Interferogram of an etch cleavage.

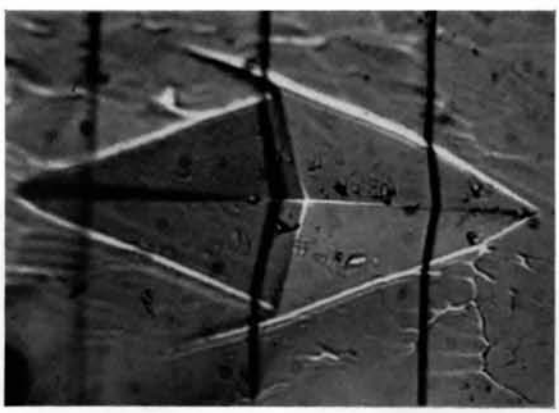

Fig. 6. A point-pyramidal pit.

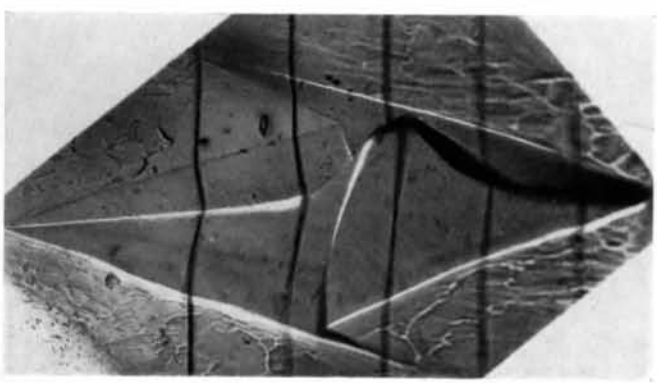

Fig. 7. A curl-bottomed pit.

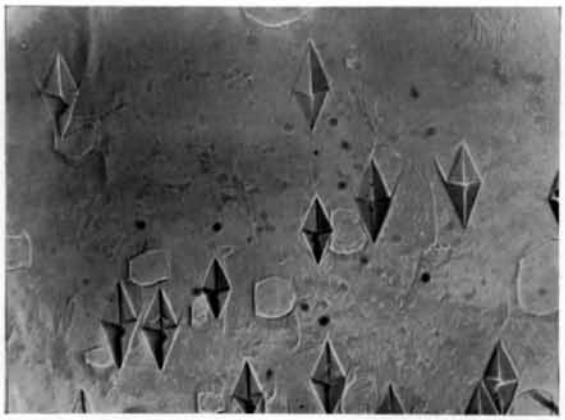

(*a*)

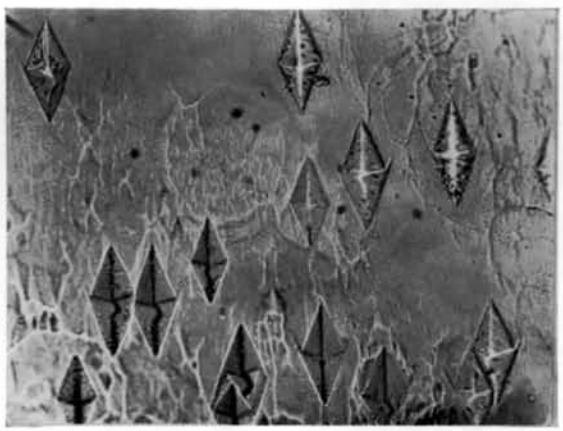

(*b*)

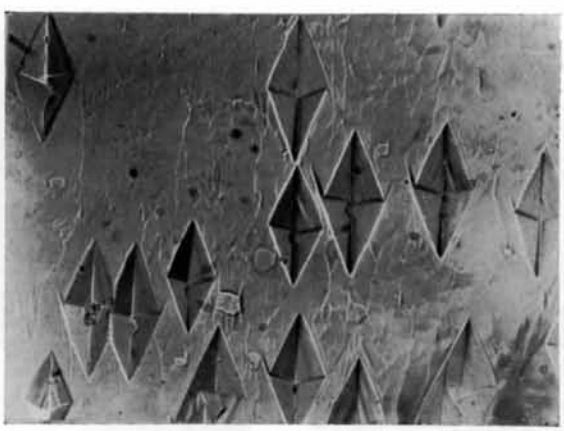

(*c*)

Fig. 8. (*a*), (*b*), (*c*) Successive stages in the development of point-pyramidal and curl-bottomed pits.

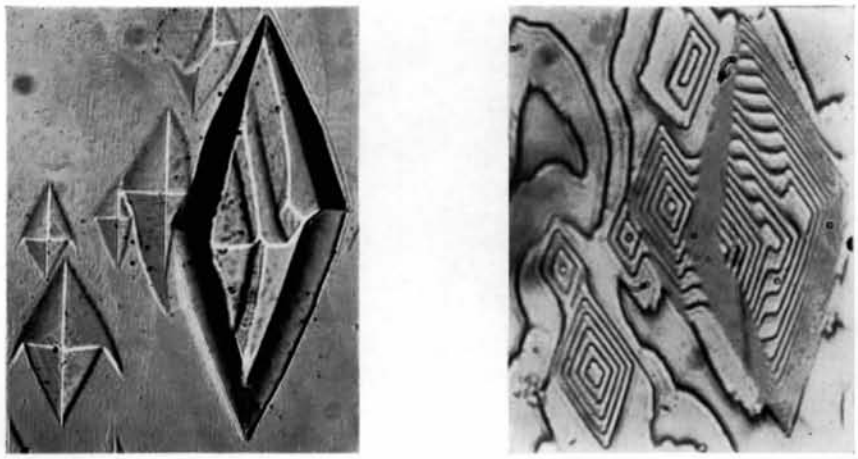

(*a*) (*b*)

Fig. 9. (*a*) An etched region showing point-pyramidal pits. (*b*) An interferogram of the region shown in (*a*).

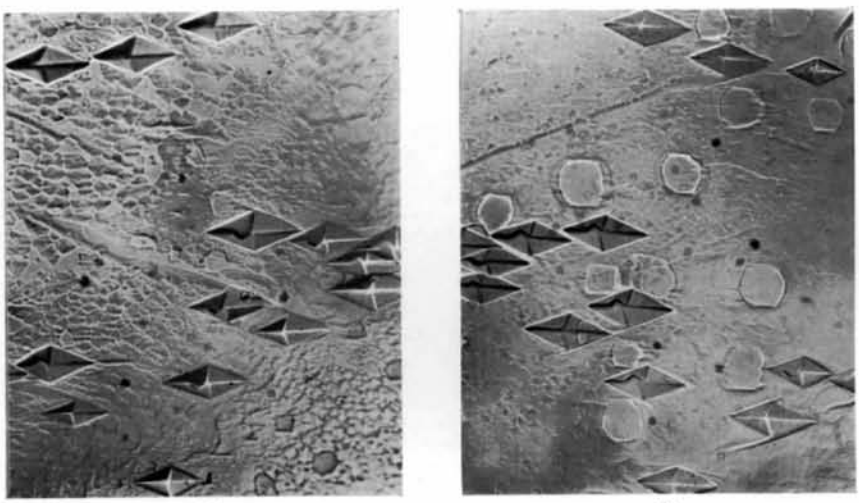

(*a*) (*b*)

Fig. 10. Etch patterns on a matched cleavage of topaz.

(*a*) (*b*)

Fig. 11. Etch patterns on matched cleavages with wings associated with them.

(*g*) The pits of smaller size continue to be relatively smaller at all stages of etching.

In order to investigate the cause of asymmetry (*r*), (*i.e.* the displacement of the point bottom of the pit from its geometrical centre) produced in point-pyramidal pits, a number of such pits were investigated in detail and numerical measurements were made at a magnification (*m*) of ×70 on them. Measurements made on some of such pits are given in Table 1.

Table 1. *Measurements of asymmetry in point-pyramidal etch pits*

Pit No.	Period of etching	Depth of pit (*d*)	Observed asymmetry (*r*)	Ratio *d*/*r*	$\theta = \tan^{-1} md/r$
	30 sec	1·0 μ	0·015 cm	0·47	25°
1	60	1·7	0·025	0·47	25° 27′
	90	2·1	0·030	0·49	26° 12′
	30	1·0	0·015	0·47	25°
2	60	1·6	0·023	0·48	25° 56′
	90	2·1	0·031	0·47	25° 24′
	30	0·95	0·014	0·47	25° 25′
3	60	1·6	0·023	0·48	25° 56′
	90	2·1	0·030	0·49	26° 12′
	30	1·0	0·015	0·47	25°
4	60	1·7	0·025	0·48	25° 27′
	90	2·2	0·032	0·48	25° 42′
	30	1·0	0·014	0·50	26° 32′
5	60	1·6	0·024	0·47	25°
	90	2·15	0·031	0·48	25° 50′
	30	0·95	0·014	0·47	25° 24′
6	60	1·5	0·022	0·47	25° 30′
	90	2·0	0·028	0·49	26° 28′

The fact that the pits remain point-pyramidal at every stage of etching may be due to their origin at the sites of dislocations in the crystal. It is quite clear from Table 1 that with the increase in the time of etching the pits grow in size, their depth increases,, and the asymmetry observed also increases. However, the ratio of the depth of the pit to the asymmetry measured always remain nearly the same for all such pits. This, therefore, led us to think that if the surface dissolution is assumed to be constant, the tips of the pits follow continuous lines as they are etched progressively deeper. The constant ratio of the depth of the pit to the asymmetry measured suggests that the dislocations at which these pits are nucleated are inclined to the cleavage face and the angle of inclination, as given in the last column of Table 1, is about 25° 30′. It is conjectured that the curl-bottomed pits might reveal the sites of the screw dislocations in the crystal lattice as shown by Gilman & Johnston (1956) for lithium fluoride and by Mendelson (1961) for sodium chloride crystals. Fig. 9(*b*) is a multiple-beam interferogram taken on the region of Fig. 9(*a*). The interferogram clearly reveals the structure of the pits seen in Fig. 9(*a*). It is seen that in the case of a point-bottomed pit, the contours are quite uniform and equally spaced, and thus suggests that the pit is bounded by four plane faces having uniform slope. The large pit is formed by the interference of more than one pit, hence the contours are quite complicated. The depths of the pits in the figure vary from 0·77 μ to 5·25 μ.

Etching of matched cleavage faces

The above observations were further extended to the etch patterns produced on the matched faces of topaz. Thus Figs. 10(*a*) and (*b*) and 11(*a*) and (*b*) represent etch patterns of matched cleavage faces. The correspondence in the number, positioning, size and orientation of the pits is in accordance with those observed by Gilman & Johnston (1956) in lithium fluoride, Mendelson (1961) in sodium chloride, by Patel & Tolansky (1957) in diamond and mica, and by Patel & Goswami (1962) in calcite crystals. Careful examination of etch patterns on the matched faces reveals the following features:

(1) A pit of smaller size corresponds to a pit of similar size on the matched face.

(2) The correspondence is also observed in regard to the asymmetry produced in the point-pyramidal pits. In matched pairs of such pits, it can clearly be distinguished that the point bottoms producing the asymmetry are displaced in one direction in one pit and in the opposite direction in the corresponding matched pit. These observations confirm our conjecture that these pits nucleate at the terminations of inclined linear dislocation lines which are cut into two by the cleavage.

(3) The correspondence also exists in the curl-bottomed pits. If the bend produced in one curl-bottomed pit is in one direction, its matched pit has a bend in the opposite direction.

(4) Correspondence is also observed in the wings produced by the extension of the sides of an etch pit. If in a pit a wing is produced by the extension of one of its sides, in its matched pit a similar wing is produced by the extension of its opposite sides in the same crystallographic direction.

(5) Sometimes, as is seen in Fig. 10, a micro-disc pattern is also produced by etching, which has no correlation on matched faces (Patel & Goswami, 1962).

Etch patterns on the opposite sides of a thin plate

Figs. 12(*a*) and (*b*) and Figs. 13(*a*) and (*b*) both show the etch patterns on the two sides of the same portion of a topaz plate 0·5 mm thick. Quite a considerable amount of correspondence in the etch patterns can clearly be observed in these photographs. The asymmetry produced in the pits on one side is in one direc-

tion, while it is produced in the reverse direction in the case of pits on the other side. In Fig. 13 a curl-bottomed pit is seen having a corresponding similar type of pit on the other face. In addition to this, correspondence is also observed in the wings produced to some pits. The observations of etch patterns on the opposite sides of a thin plate also support our conjecture regarding the existence of inclined dislocation lines in the crystal lattice.

The stratigraphy of cleaved plates

Fig. 14 shows a striking linear etch pattern on a (001) cleavage face of topaz. This pattern consists of a clearly strictly oriented region separated through having distinctive regions of different degrees of attack by the etchant. In Fig. 15 a similar etch pattern is seen crossing a large cleavage step. The displacement in the rectilinear etch pattern in crossing the cleavage step is quite distinctively seen. Such displacements of the rectilinear etch patterns across five steps of different magnitudes were measured, and the corresponding step heights were also calculated by light-profile microscopy (Tolansky, 1952) and were checked by the depth of focus method. These observations are given in Table 2.

Table 2. *Displacement of rectilinear etch patterns across cleavage steps*

Observation no.	Step height (h)	Shift in the pattern (d)	Magnification (m)	Angle calculated $\theta = \tan^{-1}(\Delta m \times h/d)$
1	9·0 μ	0·16 cm	180	45° 18′
2	14·0	0·25	350	44° 30′
3	70·0	0·63	90	45°
4	72·0	0·65	90	44° 54′
5	70·0	0·22	33	46° 24

These steps were selected on the different sides of the rectilinear etch patterns of Fig. 15. From the nature of the displacements of these rectilinear traces across the cleavage steps, it is conjectured that they may be due to:

(1) Intersection of some weak planes deposited during growth with the cleavage face.
(2) The slip produced by plastic deformation.

That the etch patterns produced on these traces match on the opposite sides of a thin topaz flake suggests that they are due not to the second alternative but to the first one. It is therefore conjectured that, as shown in the case of diamond by Patel & Tolansky (1957), and in the case of calcite by Patel & Goswami (1962), these traces may be due to deposition of some weak planes. In order to find out which planes in topaz give such rectilinear traces by the intersection with the (001) cleavage plane, the angle made by these planes with the cleavage face was calculated from the shift of these traces across large cleavage steps by the same method as reported by Patel & Goswami (1962) in the case of calcite. The calculated angles are shown in the last column of Table 2. That there is correspondence in the rectilinear etch patterns on the two sides of a large cleavage step led us to investigate such etch patterns on the opposite sides of thin flakes of topaz. Thus Figs. 16(*a*) and (*b*) represent the etch patterns on the opposite sides of a topaz flake of 0·3 mm thickness. A considerable amount of correspondence in the rectilinear etch patterns of the two sides is clearly seen. It is therefore quite clear that the planes responsible for the rectilinear etch pattern sometimes run right through the body of the crystal and hence produce similar etch patterns on the opposite sides of a thin flake of topaz when etched.

Conclusion

Fig. 14, 15 and 16 reveal that the stratigraphical etch patterns go right through the body of the crystal, and thus the etch reveals the true history of growth of topaz. The stratigraphical planes are inclined at an angle of about 45° with the cleavage face. In the case of topaz, the (111) pyramidal faces make an angle of 45° with the basal (001) cleavage face. It is therefore conjectured that during crystal growth some sheet layers might have been deposited on (111) faces. In fact the topaz crystal selected for this investigation had a large (111) pyramidal face of optical flatness. The origin of the rectilinear etch pattern is now clear. The crystal might have grown by sheet layer formation by deposition of layers on various faces of topaz. These sheets are cut by the cleavage plane and the intersection of these two planes leaves rectilinear traces on it. These rectilinear traces are revealed when the cleavage is etched, owing to preferential etching. The sheets of specific character have different thicknesses. One sheet may be relatively free from defects and may be followed by one densely populated with defects. Many of the sheets maintain their individuality right through the crystal block. In fact the characteristics of the sheets will depend upon the factors controlling the growth.

References

Billington, D. S. & Crawford, J. H. (1961). *Radiation Damage in Solids*. Princeton Univ. Press.

Gevers, R. (1953). *J. chim. phys.* **50**, 321.

Gilman, J. J. & Johnston, W. G. (1956). *J. Appl. Phys.* **27**, 1018.

Mendelson, S. (1961). *J. Appl. Phys.* **32**, 1579.

Patel, A. R. & Ramanathan, S. (1962). *Acta Cryst.* **15**, 860.

Patel, A. R. (1961). *Physica*, **27**, 1097.

Patel, A. R. & Goswami, K. N. (1962*a*). *Acta Cryst.* **15**, 47.

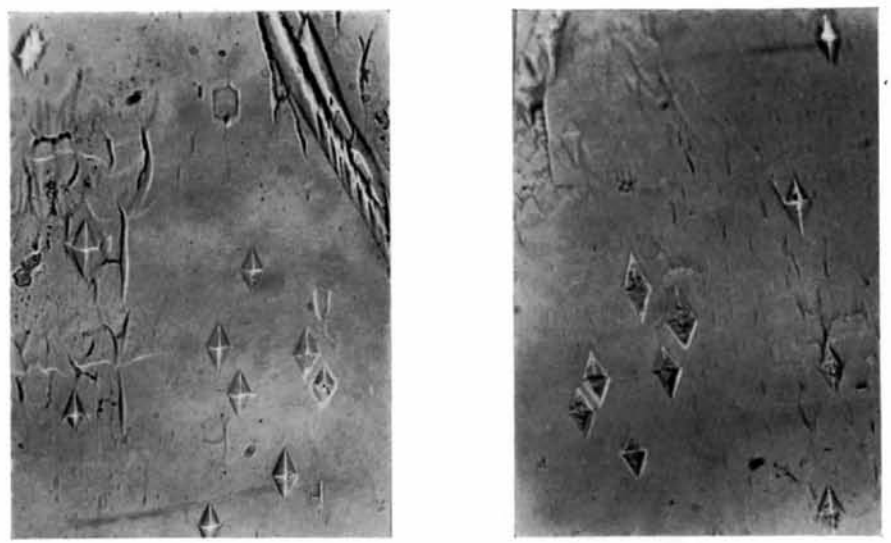

(*a*) (*b*)

Fig. 12. The etch patterns on the opposite sides of a thin flake of topaz.

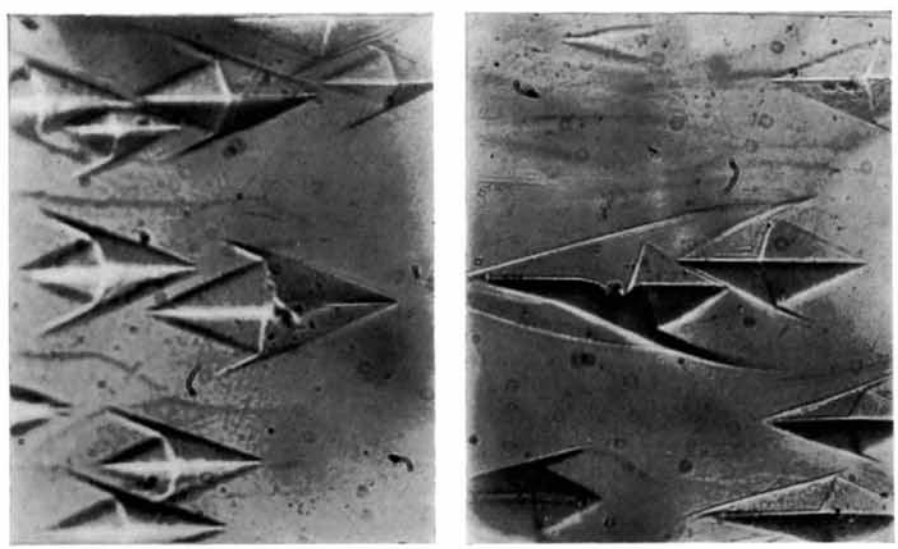

(*a*) (*b*)

Fig. 13. The etch patterns on the opposite sides of another cleavage.

[*To face p.* 572

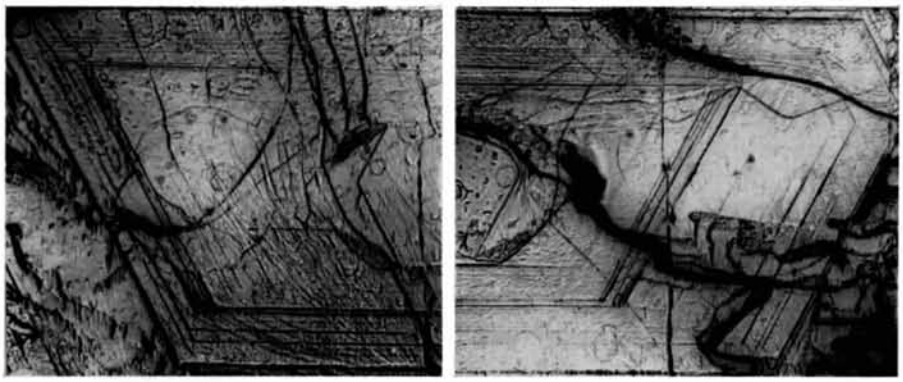

Fig. 14. The stratigraphical character of the etch pattern.

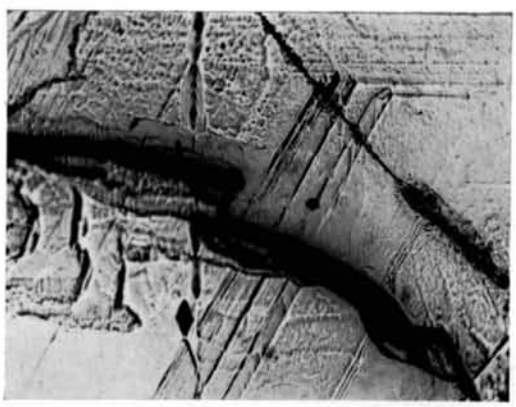

Fig. 15. Displacement of an etch pattern across a large cleavage step.

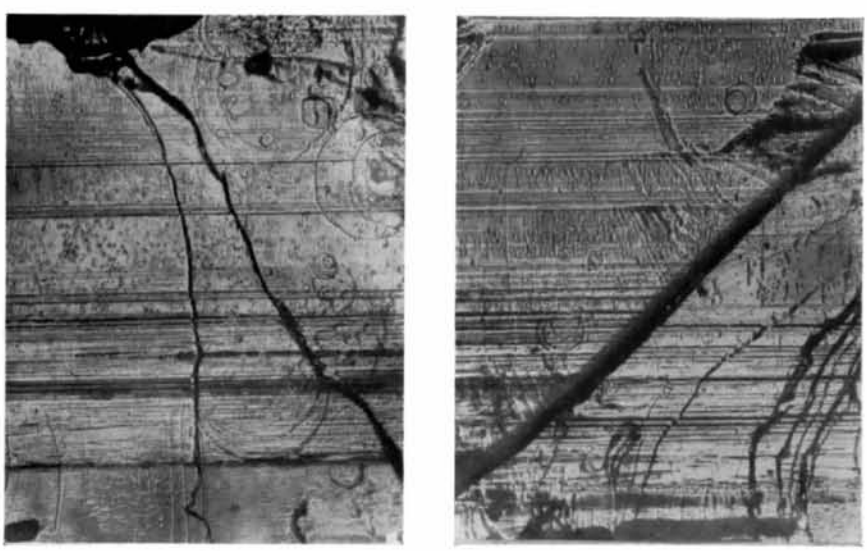

(*a*) (*b*)

Fig. 16. Matching of the stratigraphical pattern on the opposite sides of a thin flake of topaz.

PATEL, A. R. & GOSWAMI, K. N. (1962*b*). *Proc. Phys. Soc.* **79**, Part 4.
PATEL, A. R. & TOLANSKY, S. (1957). *Proc. Roy. Soc.* A, **243**, 41.
TOLANSKY, S. (1948). *Multiple Beam Interferometry of Surfaces and Films*. Oxford: Clarendon Press.
TOLANSKY, S. (1952). *Z. Electrochem.* **56**, 263.

Acta Cryst. (1964). **17**, 573

A Neutron Diffraction Study of 2-Nitrobenzaldehyde and the C–H · · · O Interaction*

BY PHILIP COPPENS†

Chemistry Department, Brookhaven National Laboratory, Upton, Long Island, New York, U.S.A.

(*Received* 20 *September* 1962 *and in revised form* 8 *July* 1963)

The structure of the stable modification of 2-nitrobenzaldehyde has been redetermined by means of neutron diffraction. Non-hydrogen atom parameters agree with values from the X-ray determination. The parameters of the hydrogen atoms are obtained. C–H · · · O interactions are discussed and it is concluded that the observed geometry of the molecule indicates the absence of an internal hydrogen bond in 2-nitrobenzaldehyde.

Introduction

The previously reported X-ray analysis of the stable modification of *o*-nitrobenzaldehyde (Coppens & Schmidt, 1964) has shown that the two substituents in this compound are not coplanar with the aromatic ring. This suggested that no hydrogen bond exists between the C–H of the aldehyde group and the oxygen of the nitro group, though various authors have interpreted their experimental results as providing evidence for the existence of such a bond. Since the X-ray analysis did not produce a reliable position for the aldehydic hydrogen atom, no definite conclusion could be drawn. In addition the aldehydic hydrogen atom plays a part in the photochemical rearrangement of *o*-nitrobenzaldehyde to nitrosobenzoic acid and its position will throw light on the mechanism of this reaction. Therefore a single-crystal neutron diffraction investigation was undertaken.

Experimental

Small crystals of *o*-nitrobenzaldehyde can be grown from alcohol–water mixtures. When such a crystal is immersed, at the end of a silk thread, in the slightly undercooled melt of *o*-nitrobenzaldehyde it grows slowly. When the melt is kept at 42·5 °C (melting point 43 °C) for about three weeks crystals are obtained of dimensions suitable for neutron diffraction with the flux available at the Brookhaven Graphite reactor (in-pile flux about $2 \cdot 10^{13}$ cm^{-2} sec^{-1}).

Two crystals with dimensions $0 \cdot 9 \times 0 \cdot 5 \times 12 \cdot 0$ mm and $1 \cdot 1 \times 2 \cdot 1 \times 12 \cdot 5$ mm were used to collect *h0l* data, the weaker reflections being collected from the larger crystal. (Both crystals were elongated in the direction of the *b* axis, but the smaller one showed the form {101}, while on the larger one the forms {001} and {100} were developed. The first two of the dimensions describing the crystals refer to directions perpendicular to the planes of these forms.) The larger crystal was then cut and a fragment with dimensions $1 \cdot 1 \times 2 \cdot 1 \times 4 \cdot 0$ mm was used to collect *hk*0 and 0*kl* intensities.

The crystals are photosensitive and have a high vapor pressure at room temperature, therefore they were inserted in silica tubes blackened with carbon black. (Both silica and carbon black are sufficiently transparent to neutrons.)

The crystallographic constants as determined by X-rays were used throughout, they are:

$$a = 11 \cdot 37,\ b = 3 \cdot 960,$$
$$c = 7 \cdot 57 \text{ Å};\ \beta = 90° 11',$$

space group $P2_1$. In the *h0l*, *hk*0 and 0*kl* zones reflections were observable up to 2θ values of 110°, 90° and 80° respectively ($\lambda = 1 \cdot 07$ Å). Within these three ranges there are 319, 69, and 38 non-symmetry-related reciprocal lattice points; 136 *h0l*, 40 *hk*0 and 20 0*kl* reflections were strong enough to be observed.

Data reduction and refinement

The data were corrected for absorption with Hamilton's program for the IBM 704 (Hamilton, 1957) ($\mu = 1 \cdot 13$ cm^{-1}). Standard deviations of the intensities were calculated with the formula:

$$\sigma^2(I_{\text{corr}}) = \Delta^2_{\text{stat}} + c_1^2 I^2 + c_2^2 (I_{\text{corr}} - I)^2$$

in which Δ_{stat} is the error due to counting statistics,

* Research performed under the auspices of the U.S. Atomic Energy Commission.

† Present address: Department of X-ray Crystallography, Weizmann Institute of Science, Rehovoth, Israel.